Electronic Supplementary Information

A synergistic electrochemical approach of boron doped carbon/cobalt pyrophosphate//MXene for high performance all solid-state asymmetric device.

Abhisek Padhy, [a, b] Rutuparna Samal,[c] Chandra Sekhar Rout [c] and J. N. Behera [a, b*]

[a] *National Institute of Science Education and Research (NISER), 'An OCC of Homi Bhabha National Institute', Jatni, Khordha 752050, Odisha, India*
[b] *Centre for Interdisciplinary Sciences (CIS), NISER, Jatni 752050, Odisha, India*

[c] *Centre for Nano and Material Sciences, Jain Global Campus, Ramanagaram, Bangalore562112, India*

*Email: jnbehera@niser.ac.in

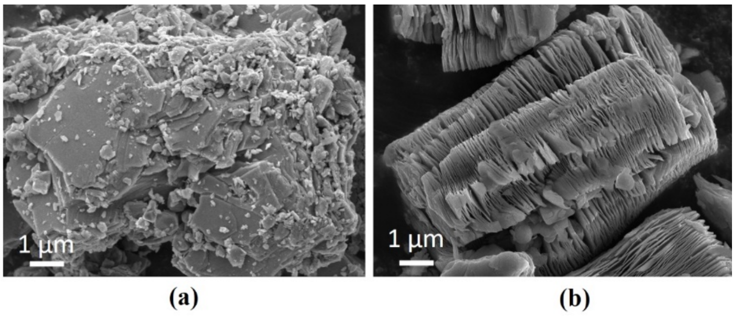

Fig. S1 FESEM images of (a) MAX (Ti_3AlC_2) and (b) MXene (Ti_3C_2).

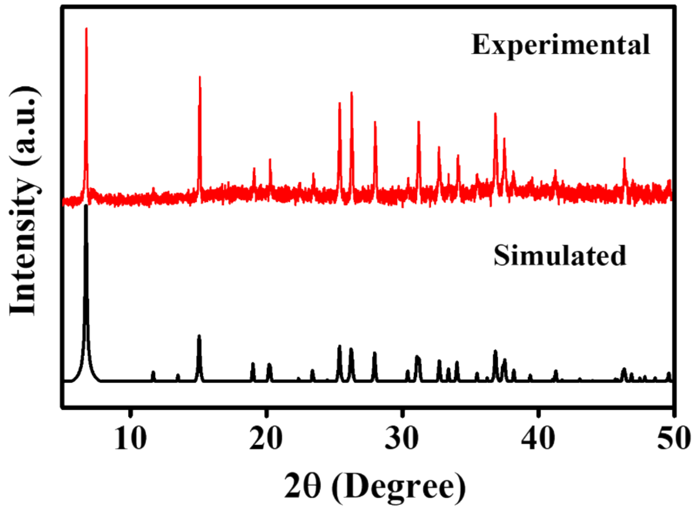

Fig. S2 Simulated pattern of the open framework along with the experimental pattern before and after boron incorporation.

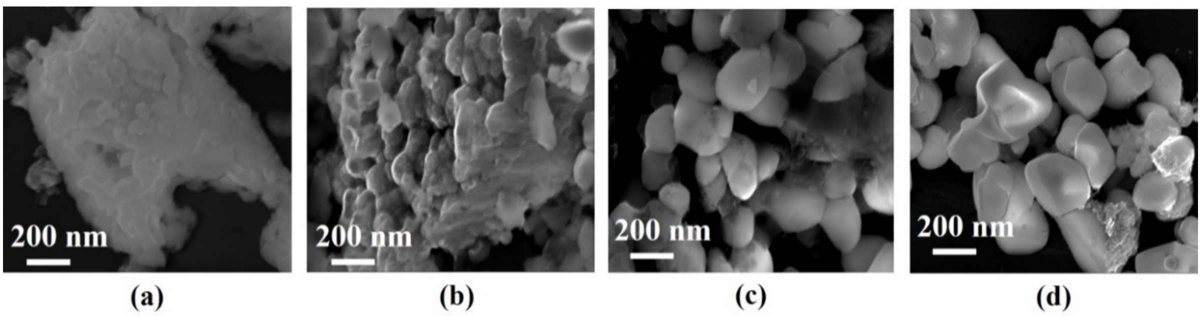

Fig. S3 SEM images of pristine (a) GC@CPP, (b) B-GC@CPP-2, (c) B-GC@CPP-4, (d) B-GC@CPP-8. There occurs a small reduction in the agglomeration with increase in boron quantity during synthesis.

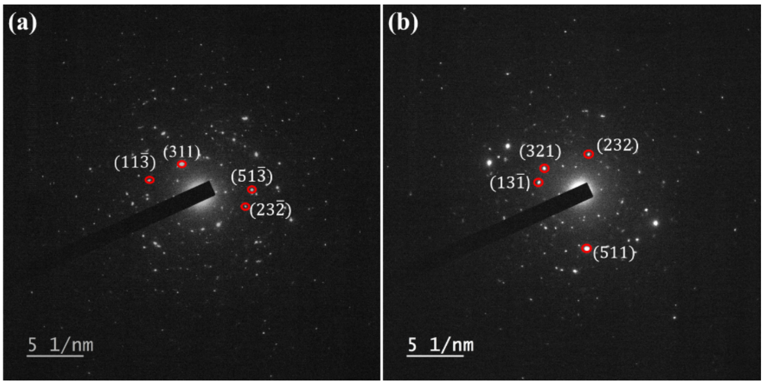

Fig. S4 SAED pattern of (a) GC@CPP, (b)B-GC@CPP-4

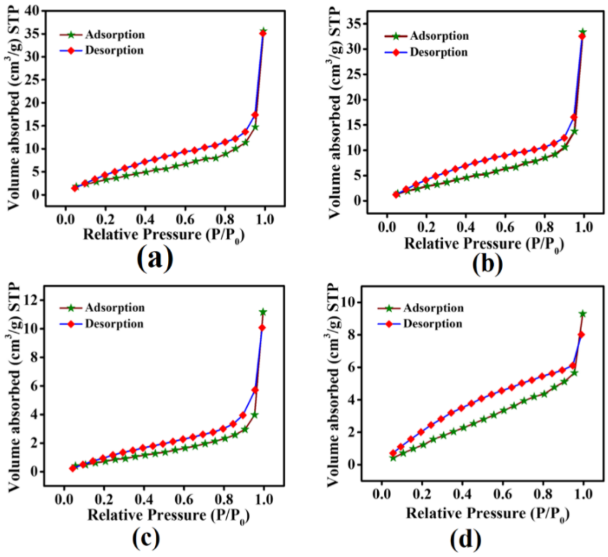

Fig. S5 Adsorption/desorption isotherm for (a) Pristine GC@CPP, (b) B-GC@CPP-2, (c) B-GC@CPP-4, (d) B-GC@CPP-8.

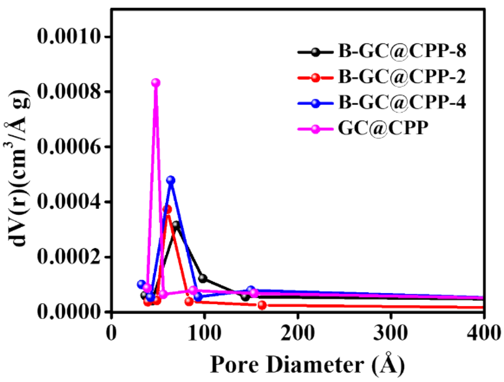

Fig. S6 BJH pore size distribution curves GC@CPP, B-GC@CPP-2, B-GC@CPP-4, B-GC@CPP-8.

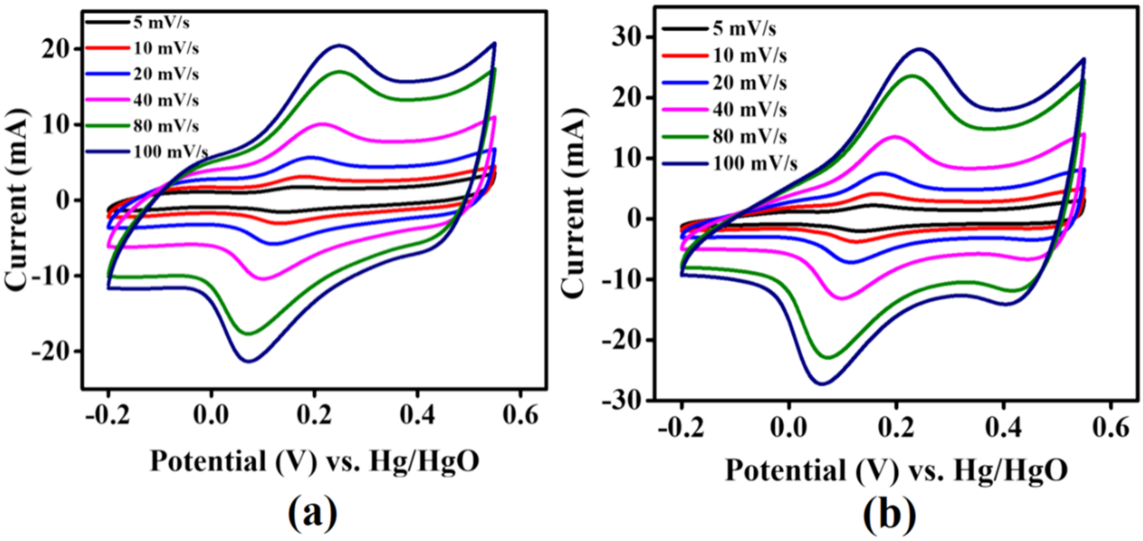

Fig. S7 (a) CV curves of B-GC@CPP-2, (b) CV curves of B-GC@CPP-8.

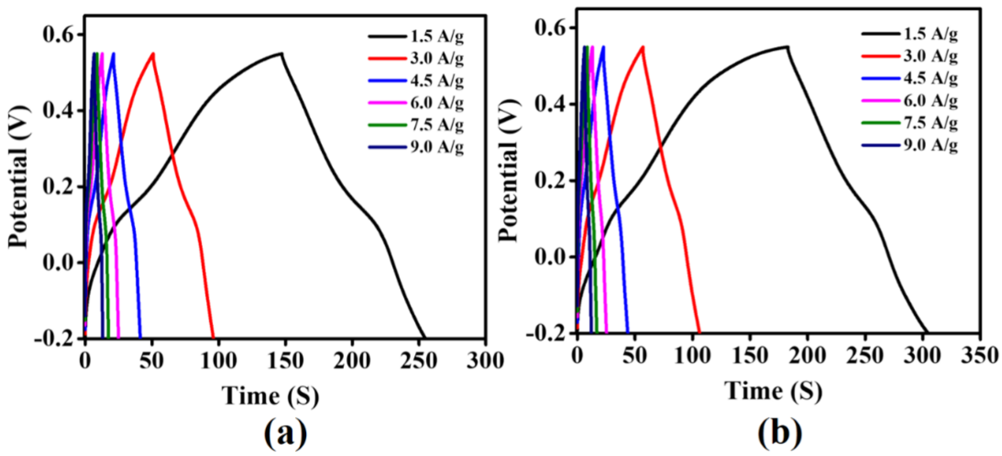

Fig. S8 (a) GCD profiles of B-GC@CPP-2, (b) GCD profiles of B-GC@CPP-8.

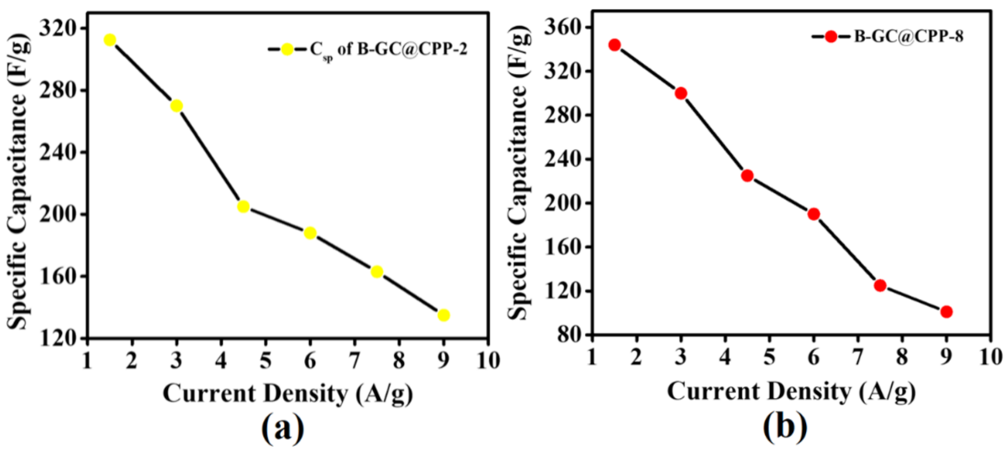

Fig. S9 Specific capacitance at different current density for (a) B-GC@CPP-2, (b) GCD profiles of B-GC@CPP-8.

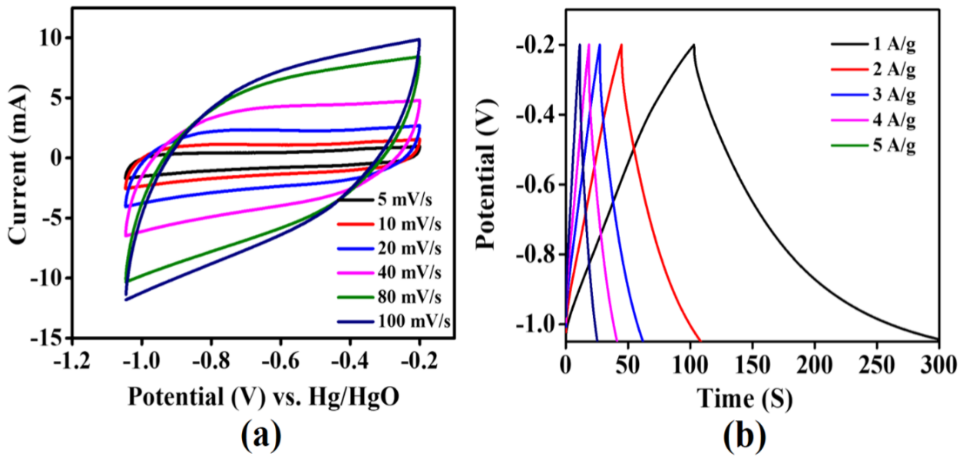

Fig. S10 (a) CV curves of MXene (Ti_3C_2), (b) GCD profiles of MXene.

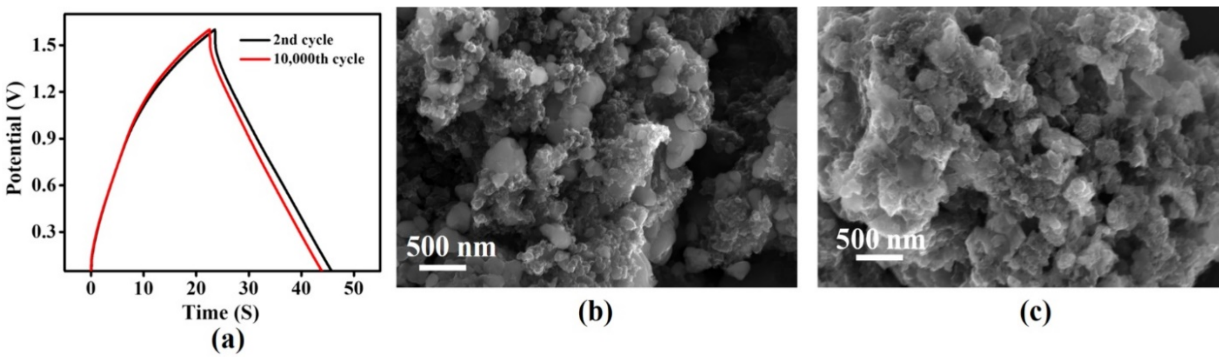

Fig. S11 (a) GCD profiles of the material in two-electrode ASC before and after 10,000th cycle, SEM image of B-GC@CPP-4 along-with acetylene black and PVDF (b) before cycling (c) after cycling.

Table S1: Comparison table for phosphate-based material.

Name	Specific Capacitance	Potential window	Sp. cap. of ASC	Energy density	Power density	Capacitance retention & Cycle No.s	Ref.
Flower like 3D $Co_3(PO_4)_2.8H_2O$	350 F/g at 1A/g (3 M KOH)	0 – 0.42 V	-	-	-	102% retention after 1000 cycles	1
Binder free $Co_3(PO_4)_2$ 1D nanograss	12,285 mF/cm^2 at 5 mV/s (1 M KOH)	0 – 0.7 V	85 F/g at 1A/g	26.66 Wh/kg	750 W/kg	80% retention after 6000 cycles (Device)	2
$Co_2P_2O_7$ nano/microstructures	367.2 F/g at 0.625 A/g (3 M KOH)	0 – 0.4 V	-	-	-	96.2% retention after 3000 cycles	3
$CoHPO_4.3H_2O$ ultrathin nanosheets	413 F/g at 1.5 A/g (3 M KOH)	0 – 0.45 V	-	-	-	>85.1% retention after 3000 cycles	4
1D $Co_2P_2O_7$ nanorods	483 F/g at 1 A/g (3 M KOH)	-0.1 – 0.45 V	-	-	-	90% retention after 3000 cycles	5
Amorphous $Co_{0.2}Ni_{0.8}$ polyphosphate	1259 F/g at 1.5 A/g (3 M KOH)	0 – 0.55 V	119 F/g at 1 A/g	42.4 Wh/kg	800 W/kg	80% retention after 2000 cycles (Device)	6
$Ni_3P_2O_8$ - $Co_3P_2O_8.8H_2O$	1974 F/g at 0.5 A/g (6 M KOH)	0 – 0.4 V	94 F/g at 0.5 A/g	33.4 Wh/kg	399 W/kg	83% retention after 5000 cycles (Device)	7
$Co_2P_2O_7$ Nanosheets	580 F/g at 1 A/g in 0.1 M KFC ($K_3Fe(CN)_6$) in 3 M KOH	-0.2 – 0.48 V	-	-	-	96% retention upto 5000 cycles	8
Nanoporous Nickel phosphate	265 F/g at 20 mV/s (3 M KOH)	0 – 0.5 V	-	-	-	97% retention after 1000 cycles	9

$Co_{0.4}Ni_{1.6}P_2O_7$/N-doped graphene (NG) composites	1473 F/g at 1 A/g (3 M KOH)	0 – 0.55 V	-	34.9 Wh/kg	800 W/kg	70% retention after 5000 cycles (device)	10
sodium doped $Ni_2P_2O_7$-$Co_2P_2O_7$	295.2 Cg^{-1} at 2 A/g (3 M KOH)	0 – 0.45 V	-	54.1 Wh kg^{-1}	1700 W kg^{-1}	95% retention after 2000 cycles (device)	11
Boron doped carbon/cabalt pyrophosphate hybrid	**395.1 F/g at 1.5 A/g (3 M KOH)**	**-0.2 – 0.55 V**	**125 F/g at 2 A/g**	**45 Wh/kg**	**1735 W/kg**	**96% retention after 10,000 cycles (device)**	**This work**

References

1 H. Li, H. Yu, J. Zhai, L. Sun, H. Yang and S. Xie, *Mater. Lett.*, 2015, **152**, 25–28.

2 K. V. Sankar, S. C. Lee, Y. Seo, C. Ray, S. Liu, A. Kundu and S. C. Jun, *J. Power Sources*, 2018, **373**, 211–219.

3 H. Pang, Z. Yan, Y. Ma, G. Li, J. Chen, J. Zhang, W. Du and S. Li, *J. Solid State Electrochem.*, 2013, **17**, 1383–1391.

4 H. Pang, S. Wang, W. Shao, S. Zhao, B. Yan, X. Li, S. Li, J. Chen and W. Du, *Nanoscale*, 2013, **5**, 5752–5757.

5 L. Hou, L. Lian, D. Li, J. Lin, G. Pan, L. Zhang, X. Zhang, Q. Zhang and C. Yuan, *RSC Adv.*, 2013, **3**, 21558–21562.

6 C. Chen, N. Zhang, Y. He, B. Liang, R. Ma and X. Liu, *ACS Appl. Mater. Interfaces*,

2016, **8**, 23114–23121.

7 M. C. Liu, J. J. Li, Y. X. Hu, Q. Q. Yang and L. Kang, *Electrochim. Acta*, 2016, **201**, 142–150.

8 Z. Khan, B. Senthilkumar, S. Lim, R. Shanker, Y. Kim and H. Ko, *Adv. Mater. Interfaces*, 2017, **4**, 1700059.

9 M. Pramanik, R. R. Salunkhe, M. Imura and Y. Yamauchi, *ACS Appl. Mater. Interfaces*, 2016, **8**, 9790–9797.

10 P. Sun, Z. Li, L. Zhang, C. Dong, Z. Li, H. Yao, J. Wang and G. Li, *J. Alloys Compd.*, 2018, **750**, 607–616.

11 C. Wei, S. Yang, W. Liu, X. Hou, Y. Sun, J. Zhao, W. Xiong, C. Cheng and D. Zhang, *Appl. Surf. Sci.*, 2019, **465**, 763–771.